Localization and clustering in the nuclear Fermi liquid

J.-P. Ebran,[1] E. Khan,[2] T. Nikšić,[3] and D. Vretenar[3]

[1]*CEA/DAM/DIF, F-91297 Arpajon, France*
[2]*Institut de Physique Nucléaire, Université Paris-Sud, IN2P3-CNRS, F-91406 Orsay Cedex, France*
[3]*Physics Department, Faculty of Science, University of Zagreb, 10000 Zagreb, Croatia*

Using the framework of nuclear energy density functionals we examine the conditions for single-nucleon localization and formation of cluster structures in finite nuclei. We propose to characterize localization by the ratio of the dispersion of single-nucleon wave functions to the average internucleon distance. This parameter generally increases with mass and describes the gradual transition from a hybrid phase in light nuclei, characterized by the spatial localization of individual nucleon states that leads to the formation of cluster structures, toward the Fermi liquid phase in heavier nuclei. Values of the localization parameter that correspond to a crystal phase cannot occur in finite nuclei. Typical length and energy scales in nuclei allow the formation of liquid drops, clusters, and halo structures.

Nucleons in atomic nuclei and extended nuclear matter exhibit a variety of phases. Liquid drop aspects, for instance, were first inferred [1] from fission properties in heavy nuclei. Soon afterwards it was also predicted and observed that cluster states could occur, especially in light nuclei [2]. Halo structures in nuclei were discovered in the late 1980s [3]. Although a number of theoretical models have been developed that successfully describe particular features of these nucleonic phases, open questions remain: Can nucleon crystal states occur? Do all nucleonic phases (liquid, cluster, halo, crystal) have a common origin and, therefore, can they be described in a unified theoretical framework? In particular, in a recent study [4] we have shown that the confining nuclear potential determines the degree of localization and clustering in finite nuclei. In the present work we analyze the emergence of cluster states, considered as a transitional phase between a quantum liquid (nuclear matter) and a solid (crystal). These considerations are also relevant for the description of the crust of neutron stars, where it is known that decreasing matter density (further from the center of the star) leads to a transition from the nuclear matter phase (liquid) to a Wigner crystal, with a pasta (cluster) phase in between [5–7].

Clustering, the arrangement of nucleons in clusters of bosonic characters, especially in light nuclei, coexists with the nuclear mean-field. The nature of the cluster phase itself is very much under debate: Can nuclei in the cluster phase behave like a dilute gas of α particles [8–10]? This refers to the localization of the α's with respect to the size of the nucleus. Here we first address the question of localization of nucleons: What is the mechanism of confinement of individual nucleons into clusters such as, for instance, α particles? Because the majority of theoretical approaches that quantitatively describe cluster states assume *a priori* the existence of such structures (or facilitate their formation by employing Gaussian wave functions centered at given positions in space), and the corresponding effective interactions are adjusted to the binding energies and scattering phase shifts of these configurations, one cannot say that the initial localization of nucleons and the mechanism that drives the transition from the fermionic liquid

to cluster structures are fully understood [11]. As shown in our previous study [4], there is a direct correlation between the effective potential that confines the neutrons and protons to the nucleus, and the enhancement of the symmetries of the clustering. The deformation of the nucleus also contributes to the formation of clusters because it removes the degeneracy of single-nucleon levels associated with spherical symmetry [2]. Clustering effects are, of course, more dominant in excited nuclear states, and this can be understood from the fact that the closeness to the particle emission threshold favors cluster formation. States close to the continuum cannot be isolated from the environment of scattering states, so cluster states at the threshold belong to an open quantum system [12]. The origin of cluster formation, however, lies in the effective nuclear interaction, and a fully microscopic description of clustering necessitates a framework that encompasses both cluster and quantum liquid-drop aspects in light and heavier nuclei [4,13].

The issue of solid (crystal) vs quantum liquid nature of nuclei was addressed by Mottelson, who emphasized that the essence of the concept of independent particle motion is the fact that the orbits of individual nucleons are delocalized and reflect the shape and radial dependence of the effective potential over the entire nucleus [14]. Mottelson used the quantality parameter [15],

$$\Lambda \hat{=} \frac{\hbar^2}{m\bar{r}^2 V_0'},\tag{1}$$

with the strength of the bare nucleon-nucleon interaction $V_0' \sim 100$ MeV and the inter-nucleon equilibrium distance $\bar{r}$, to characterize the transition between quantum liquid and crystalline solid phases. The quantality Λ is defined as the ratio of the zero-point kinetic energy of the confined particle to its potential energy, and the transition occurs in the region $\Lambda \simeq 0.1$. The typical value obtained for nuclear matter (m being the nucleon mass), $\Lambda \simeq 0.5$, is characteristic for a quantum liquid phase [14]. However, the parameter Λ is defined for infinite homogeneous systems and its

applicability to finite nuclei is limited by the fact that it does not include any nuclear mass or size dependence. Cluster states in finite nuclei introduce an additional phase of nucleonic matter. In fact, if instead of the nucleon-nucleon potential one considers an α-α potential [16] for V_0' in Eq. (1), the value of the quantality parameter decreases to $\Lambda \simeq 0.1$, entering into the liquid-to-crystal phase transition region [17].

To analyze localization and the occurrence of clustering in finite nuclei we need to consider a quantity that is sensitive to the nucleon number and size of the nucleus. Two characteristic lengths quantify the crystalline vs Fermi liquid transition, similar to the condensed-matter case [18]: the localization of the constituent wave functions in the system and the average interconstituent distance. Hence, the localization of the single-nucleon wave function, and eventually the degree of nucleonic density clustering, can be quantified by the dimensionless parameter α introduced in Ref. [4],

$$\alpha \triangleq \frac{\Delta r}{\bar{r}}, \qquad (2)$$

where $\bar{r}$ is the average internucleon distance, and Δr the spatial dispersion of the wave function:

$$\Delta r = \sqrt{\langle r^2 \rangle - \langle r \rangle^2}. \qquad (3)$$

We propose to use the parameter α to study localization effects in nuclei. For large values of α the orbits of individual nucleons will be delocalized and the nucleus in the Fermi liquid phase. However, when α is small nucleons will be localized on the nodes of a crystal-like structure. At intermediate values one expects a transition from the quantum liquid phase to a hybrid phase of cluster states. For finite systems such as nuclei this transition, of course, cannot be sharp. In a first approximation one expects that the transition occurs for $\alpha \approx 1$ because for this value the spatial dispersion of the single-nucleon wave function is of the same size as the internucleon distance and, therefore, optimal for nucleons to form a correlated cluster such as an α particle.

Localization parameters have also been considered for other quantum systems, such as quantum dots [19], or in condensed matter [20], to characterize the occurrence of a hybrid phase between the liquid and crystal phases. However, in general it will not be possible to find a universal and quantitative localization parameter that can be applied to different quantum systems, because the transition from the quantum liquid to the crystal phase is controlled by the specific dynamics and length scale of the system under consideration [19,20]. In the nuclear case, in particular, finite size effects are important. It will be shown that the parameter α can be used to qualitatively characterize transitions between different phases of nucleonic matter.

In a first, non-self-consistent, approximation one can use a three-dimensional isotropic harmonic oscillator (HO) for the confining nuclear potential. This approximation allows for a qualitative discussion of the effects of the effective nuclear interaction on the spatial arrangement of nucleons. The three-dimensional HO wave functions $\varphi_{klm}(\vec{r})$ for the first s, p, and d states, which provide the main contribution to cluster states

in light nuclei, read [21]:

$$\varphi_{0lm}(\vec{r}) \sim \frac{r^l}{b^{(3/2+l)}} e^{-\frac{r^2}{2b^2}} Y_l^m(\hat{r}), \qquad (4)$$

where b is the oscillator length defined by

$$b \triangleq \sqrt{\frac{\hbar}{m\omega_0}} = \frac{\sqrt{\hbar R}}{(2mV_0)^{1/4}}, \qquad (5)$$

where R is the radius of the potential for which $V = 0$ and V_0 denotes the depth of the potential at $r = 0$. It should be emphasized that charge radii of atomic nuclei are determined with high precision in electron scattering experiments, in contrast to the depth of a confining potential V_0 which is experimentally poorly constrained.

A straightforward calculation yields the spatial dispersion $\Delta r \approx 0.5b$ for the first s, p, and d HO wave functions, and they display a Gaussian-like radial dependence [Eq. (4)]. Consequently, for a constant radius R, a deeper potential V_0 implies a smaller value of the oscillator length b [Eq. (5)], and thus a smaller dispersion. This concept can be extended to the more general case of deformed nuclei by approximating the confining potential with an axially deformed HO. The wave functions are then expressed as [22,23]

$$\varphi_{n_r,n_z,m_l}(r, \phi, z) \sim e^{im_l} \left(\frac{r}{b_\perp}\right)^{m_l} H_{n_z}(z/b_z)$$
$$\times L_{n_r}^{m_l}(r^2/b_\perp^2) e^{-\frac{1}{2}\left(\frac{z^2}{b_z^2} + \frac{r^2}{b_\perp^2}\right)}, \qquad (6)$$

where H and L are the Hermite and Laguerre polynomials, respectively. Equation (6) displays a radial dependence similar to the three-dimensional (3D) isotropic case [Eq. (4)]: The dispersion of the wave functions depends on the oscillator lengths b_z and $b_\perp$ in the respective directions, which in turn depend on the depth of the potential. In the deformed HO approach, the depth of the potential, therefore, determines the localization of nucleon wave functions, just like in the spherical case.

The localization parameter α obtained using expression (5) for the harmonic oscillator length reads

$$\alpha \simeq \frac{b}{r_0} = \frac{\sqrt{\hbar R}}{r_0(2mV_0)^{1/4}}, \qquad (7)$$

with $r_0 = 1.25$ fm [24]. Using the liquid drop parameterization for the radius $R = r_0 A^{1/3}$, Eq. (7) reads

$$\alpha = \frac{\sqrt{\hbar} A^{1/6}}{(2mV_0 r_0^2)^{1/4}} \simeq 0.67 A^{1/6}. \qquad (8)$$

Figure 1 displays the evolution of α with A, for a typical values of $V_0 = 70$ MeV. The localization parameter α generally increases with the number of nucleons and, therefore, cluster states are more easily formed in light nuclei, as observed experimentally [2]. The transition from localized clusters to a liquid state occurs for nuclei with $A \approx 30$. For heavier systems α is considerably larger than 1 and, therefore, heavy nuclei consist of largely delocalized nucleons; this explains their liquid drop nature and the large mean free path of nucleons. More precisely, nuclei are in the Fermi liquid phase and localized cluster states (hybrid phase) can be formed in light
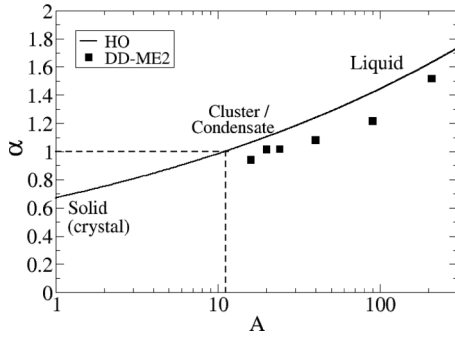
FIG. 1. The localization parameter α [Eq. (8)] as a function of the number of nucleons (solid line). The average values of α for ^{16}O ^{20}Ne, ^{24}Mg, ^{40}Ca, and ^{90}Zr, calculated for the microscopic self-consistent solutions obtained using the functional DD-ME2, are denoted by squares.

nuclei. Figure 1 also nicely illustrates the fact that a crystal phase ($\alpha \lesssim 0.8$) cannot occur in finite nuclei. However, nature may offer the possibility of existence of nucleonic crystals in the crust of neutron stars, where crystallization is caused by the long-range Coulomb interaction in a gravitationally constrained environment [6]. The transition between the Wigner crystal and the quantum liquid in the neutron star crust can be described by various models: gelification [25], Coulombic frustration [26], or quantum melting [20].

In a fully microscopic analysis, the first two columns of Table I display the values of the localization parameter α, calculated from Eq. (2) using the self-consistent ground-state solutions for the $N = Z$ nuclei ^{20}Ne, ^{24}Mg, ^{28}Si, ^{32}S, and also the heavy ^{208}Pb nucleus, obtained with the functionals SLy4 [27] and DD-ME2 [28]. These two functionals are representative of the two standard classes of nuclear energy density functionals (EDFs), the nonrelativistic and relativistic functionals, and in Ref. [4] they were used to calculate the self-consistent equilibrium mean-field solution for ^{20}Ne. Both functionals reproduce the empirical ground-state properties (binding energy, charge radius, matter radius) with a typical accuracy of 1%, as well as the quadrupole deformation of the equilibrium shape. However, as it will be also shown in this study, the density calculated with SLy4 displays a smooth behavior characteristic of a Fermi liquid, whereas

TABLE I. (Left) The localization parameter α [Eq. (2)] calculated from the fully self-consistent equilibrium solutions obtained with the EDFs SLy4 [27] and DD-ME2 [28]. (Right) The same but using the 3D harmonic oscillator approximation [Eq. (7)], for which SLy4 and DDME2 are used to determine the corresponding nuclear radii and depth of the confining potentials (see text).

	Self-consistent		HO + EDF	
	SLy4	DDME2	SLy4	DDME2
^{20}Ne	0.99	0.97	1.00	0.97
^{24}Mg	1.00	0.95	1.02	0.96
^{28}Si	0.99	0.96	1.05	1.00
^{32}S	0.99	0.96	1.06	0.99
^{208}Pb	1.28	1.31	1.46	1.40

the functional DD-ME2 predicts an equilibrium density that is much more localized, with pronounced cluster structures. The dispersions Δr correspond to the self-consistent single-nucleon Nilsson state [1101/2], which gives a pronounced contribution to clustering in these nuclei [4]. Taking $\bar{r} = 0.9$ fm as a characteristic internucleon equilibrium distance [14], we determine the corresponding values of the cluster parameter α [Eq. (2)], displayed in the first two columns of Table I. In the four lighter nuclei ^{20}Ne, ^{24}Mg, ^{28}Si, ^{32}S the α values calculated with DD-ME2 are systematically smaller than those obtained using SLy4, reflecting the more pronounced localization of the nucleonic densities that was already observed in our previous study in Ref. [4]. While for light nuclei $\alpha \leqslant 1$, in the case of ^{208}Pb α is considerably larger than 1 and this unambiguously characterizes the quantum liquid phase of nucleonic matter in this nucleus. Note that for ^{28}Si which is oblate in the equilibrium state, the dispersion is calculated for the Nilsson state [1011/2]. We have verified that similar values are obtained for other single nucleons states that build the cluster structures in these nuclei and, also, that the localization parameter α averaged over all occupied states increases with mass number.

For completeness, in the last two columns of Table I we also list the values of the localization parameter α obtained using the HO expression Eq. (7) for the dispersion. In this calculation, however, the nuclear radius R and the depth of the potential V_0 are determined microscopically using the self-consistent equilibrium solutions calculated with the EDFs SLy4 and DD-ME2. The trend is similar to that obtained in the fully microscopic calculation; that is, DD-ME2 predicts systematically smaller values of the localization parameter α. Note that this conclusion holds even when we replace the nucleon bare mass in the denominator of Eq. (7) with the effective mass m^*. The effective nucleon mass for the functional SLy4 is $0.70m$, and for DD-ME2 it is $0.66m$. In this case the value of the parameter α increases by a factor $(m/m^*)^{1/4} \simeq 1.1$, but the ratio between values that correspond to SLy4 and DD-ME2 is not altered by more than 1%.

In addition to the localization parameter obtained from the HO length [Eq. (8)], in Fig. 1 we have also included the average values of α for ^{16}O (0.94), ^{20}Ne (1.02), ^{24}Mg (1.02), ^{40}Ca (1.08), ^{90}Zr (1.22), calculated fully microscopically using the functional DD-ME2. These values are obtained by averaging the microscopic dispersions Eq. (2) for all occupied proton and neutron orbitals in the self-consistent ground-state solution and dividing by the characteristic internucleon equilibrium distance $\bar{r} = 0.9$ fm [14]. The microscopic average localization parameter describes the gradual transition from the hybrid phase, characterized by the spatial localization of individual nucleons, toward the Fermi liquid phase in heavier nuclei.

The localization of single-nucleon states can be analyzed in the HO approximation but, of course, a harmonic oscillator potential cannot give rise to clustering. Energy density functionals, however, implicitly include many-body short- and long-range correlations through their explicit density dependence and, therefore, should allow formation of clusterlike substructures [13]. Most modern EDFs, for instance, reproduce the binding energy and size of the α particle even though their parameters are not specifically adjusted to very
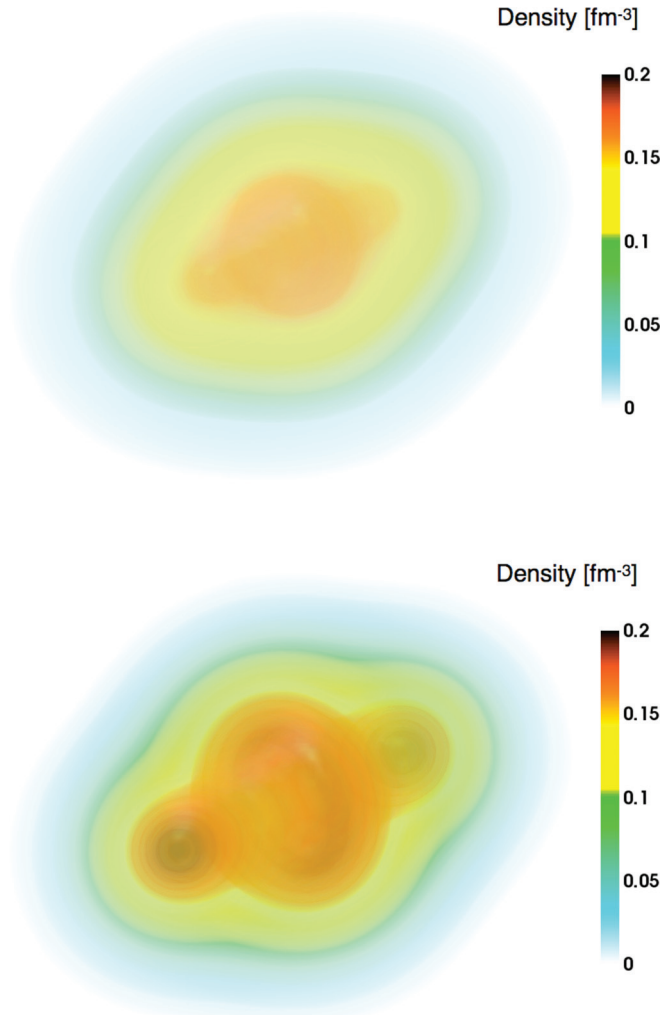
FIG. 2. (Color online) Self-consistent ground-state densities of ^{20}Ne, calculated with the EDFs SLy4 (top) and DD-ME2 (bottom). The densities (in units of fm^{-3}) are plotted in the the intrinsic frame of reference that coincides with the principal axes of the nucleus.

FIG. 3. (Color online) Same as described in the caption to Fig. 2 but for the nucleus ^{28}Si.

light nuclei. The different localization properties predicted by the functionals SLy4 and DD-ME2 are reflected in the corresponding nucleon density distributions. In Fig. 2 we display the corresponding axially and reflection symmetric self-consistent equilibrium nucleon density distributions of ^{20}Ne. Although these functionals predict similar values for the binding energy, charge and matter radii, and quadrupole deformation, the corresponding equilibrium density distributions are rather different. SLy4 yields a simple axially deformed prolate ellipsoid, with only a slight indication of possible cluster formation. DD-ME2, however, predicts two regions of pronounced localization at the outer ends of the symmetry axis and an oblate deformed core. The sharper density peaks will, of course, greatly enhance the probability of formation of α clusters in excited states. We note that a similar quasimolecular α-^{12}C-α structure, although with somewhat less pronounced clustering, was also obtained in the Hartree-Fock calculation of Ref. [13], using the SkI3 Skyrme
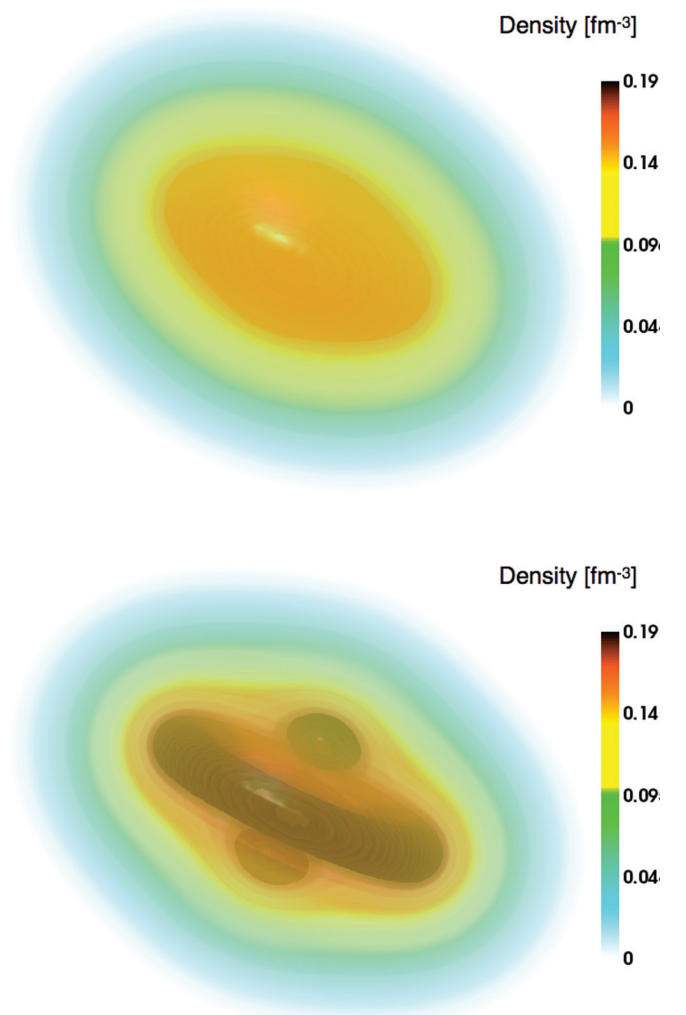
functional. Because the nucleon effective masses for the two functionals are very similar ($0.70m$ for SLy4 and $0.66m$ for DD-ME2), the different level of localization and clustering predicted by SLy4 and DD-ME2 is partly related to the depth of the corresponding confining Kohn-Sham potentials [4], similar to the HO case [Eq. (7)]. In Figure 3 we show another example, the equilibrium density distributions of ^{28}Si calculated with SLy4 and DD-ME2. In this case the equilibrium shape is oblate ($\beta \approx -0.35$), and again we find that DD-ME2 predicts the formation of clusterlike structures, whereas nucleonic density shows a smooth gradual decrease from the center of the oblate ellipsoid calculated with SLy4.

The present discussion can qualitatively be related to delocalized wave functions of halo states in light nuclei [29]. Several subtle effects are at work in halo structures, such as the inversion between the p and the s orbitals and the coupling to the continuum [30]. Here we only examine the delocalization of single-particle wave functions. When the confining nuclear potential is approximated by a square well, the oscillations of the wave function of a state of energy E (<0) are determined by the wave number $\hbar^2 k^2 = 2m(E + V_0)$, whereas outside of

the potential the decay of the wave function is governed by $\hbar^2 k'^2 = -2mE$, favoring a large radial extension for weakly bound states. However, inside the potential a larger k favors localization, and this occurs when the potential is deeper and/or E gets closer to zero. The degree of localization depends on the difference $E - (-V_0)$, and a deep potential favors the localization of the wave function for the spatial region located inside the potential. Also, a weakly bound state will be more localized, and this means that the confinement of nucleons into clusters is more likely to occur for weakly bound states close to the emission threshold. This in agreement with the Ikeda picture, as well as subsequent studies [2,8,31]. Therefore, a common feature of localized states (clusters) and halos is that

the energy of a state determines its spatial behavior either inside the potential (clusters) or outside the range of the effective potential (halo states).

An important characteristic of nuclei is that quantitatively the dispersion of the single-nucleon wave function can be of the same order of magnitude as the internucleon distance, leading to clustering as discussed above. More generally, the typical values of length scales and energies allow the formation of liquid drops, clusters, and halos in nuclei, but not crystals.

---

[1] C. F. Von Weizsäcker, Z. Phys. **96**, 431 (1935); H. A. Bethe and R. F. Bacher, Rev. Mod. Phys. **8**, 82 (1936).

[2] W. von Oertzen, M. Freer, and Y. Kanada-En'yo, Phys. Rep. **432**, 43 (2006), and references therein.

[3] I. Tanihata *et al.*, Phys. Rev. Lett. **55**, 2676 (1985).

[4] J. P. Ebran, E. Khan, T. Niksic, and D. Vretenar, Nature (London) **487**, 341 (2012).

[5] G. Baym, H. A. Bethe, and C. Pethick, Nucl. Phys. A **175**, 225 (1971).

[6] J. M. Lattimer and F. D. Swesty, Nucl. Phys. A **535**, 331 (1991).

[7] G. Watanabe, T. Maruyama, K. Sato, K. Yasuoka, and T. Ebisuzaki, Phys. Rev. Lett. **94**, 031101 (2005).

[8] A. Tohsaki, H. Horiuchi, P. Schuck, and G. Röpke, Phys. Rev. Lett. **87**, 192501 (2001).

[9] N. T. Zinner and A. S. Jensen, Phys. Rev. C **78**, 041306(R) (2008).

[10] Y. Funaki, H. Horiuchi, W. von Oertzen, G. Ropke, P. Schuck, A. Tohsaki, and T. Yamada, Phys. Rev. C **80**, 064326 (2009).

[11] M. Freer, Nature (London) **487**, 309 (2012).

[12] J. Okolowicz, M. Ploszajczak, W. Nazarewicz, Prog. Theor. Phys. Supplement **196**, 230 (2012).

[13] P.-G. Reinhard, J. A. Maruhn, A. S. Umar, and V. E. Oberacker, Phys. Rev. C **83**, 034312 (2011).

[14] B. Mottelson, in *Nuclear Structure*, edited by J. Souletie, J. Vannimenus, and R. Stora, Proceedings of the Les Houches Summer School of Theoretical Physics, LXVI, 1996 (North-Holland, Amsterdam, 1998).

[15] J. de Boer, Physica **14**, 139 (1948).

[16] F. Michel, S. Ohkubo, and G. Reidemeister, Prog. Theor. Phys. (Suppl.) **132**, 7 (1998)

[17] N. T. Zinner and A. S. Jensen, J. Phys.: Conf. Ser. **111**, 012016 (2008).

[18] D. Pines and P. Nozieres, *The Theory of Quantum Liquids* (W. A. Benjamin, New York, 1966).

[19] C. Yannouleas and U. Landman, Phys. Rev. Lett. **82**, 5325 (1999).

[20] H. Falakshahi and X. Waintal, Phys. Rev. Lett. **94**, 046801 (2005).

[21] C. Cohen-Tannoudji, B. Diu, and F. Laloe, *Mecanique Quantique* (Hermann, Paris, 1973).

[22] S. G. Nilsson, Mat.-Fys. Medd. - K. Dan. Vidensk. Selsk. **29**, 16 (1955).

[23] G. Alaga, Nucl. Phys. **4**, 625 (1957).

[24] A. Bohr and B. Mottelson, *Nuclear Structure* (Benjamin, New York, 1969).

[25] A. Coniglio *et al.*, J. Phys.: Condens. Matter **18**, S2383 (2006).

[26] P. Napolitani, Ph. Chomaz, F. Gulminelli, and K. H. O. Hasnaoui, Phys. Rev. Lett. **98**, 131102 (2007).

[27] E. Chabanat, P. Bonche, P. Haensel, J. Meyer, and R. Schaeffer, Nucl. Phys. A **635**, 231 (1998).

[28] G. A. Lalazissis, T. Niksic, D. Vretenar, and P. Ring, Phys. Rev. C **71**, 024312 (2005).

[29] P. G. Hansen and B. Jonson, Europhys. Lett. **4**, 409 (1987).

[30] K. Ikeda, T. Myo, K. Kato, and H. Toki, Lect. Notes Phys. **818**, 165 (2010).

[31] K. Ikeda, N. Tagikawa, and H. Horiuchi, Prog. Theor. Phys. (Suppl.) 464 (1968).